Internal report for Licentiate Level Seminar

Carbon Fiber Mesh as Anode for Corrosion Free Reinforced Concrete

Emma Qingnan Zhang

Department of Civil and Environmental Engineering
CHALMERS UNIVERSITY OF TECHNOLOGY
Göteborg, Sweden 2015

Abstract

Cathodic prevention technique is a promising method and has been used for the past two decades to prevent steel from corrosion in concrete structures. However, wide application of this technique has been restricted due to the high cost of anode materials. To lower the cost and further improve this technique, carbon fiber composite anode has been introduced as an alternative anode material with affordable price and other outstanding properties. Since studies and knowledge of carbon fiber composite as anode material is rare, the purpose of this work is to evaluate the feasibility of carbon fiber mesh used as anode in cathodic prevention system during the service life of at least 100 years and the effect caused by current exchange on macro- and microstructure of cementitious material. Accelerated tests were developed in order to shorten the experimental time into a manageable range. An estimation tool was used to predict the service life as well. Chemical and microstructure analyses were carried out by laser-ablation inductively-coupled-plasma mass-spectroscopy (LA-ICP-MS) and scanning electron microscope (SEM). Results indicated that Ca/Si ratio and ion distribution were changed at the current-affected zone around anode due to migration and electrochemical reactions. The predicted service life was in general longer than 100 years. Based on the results from this work it was concluded that carbon fiber mesh was suitable for the application as anode in long-term cathodic prevention system.

Keywords: cathodic prevention, carbon fiber anode, LA-ICP-MS, SEM, accelerated test, service life.

Contents

Chapter 1

Introduction

1.1 Background

Corrosion of steel reinforcement is one of the major causes of damage or deterioration of concrete structures. Conventionally, to prevent reinforcement from corrosion, low water-cement ratio (w/c) is used in concrete for reducing ingress rate of aggressive substances and large cover thickness is designed for prolonging the time for aggressive substances to reach the reinforcement steel under the specified service life. Large cover thickness simply implies more volume of concrete materials. Obviously, this conventional approach to durable concrete structures is at the sacrifice of more CO_2 emission and natural resources through consuming higher amount of cement and more constituent materials, which is against the fundamental ideas of sustainability. Although the use of industrial by-products, such as fly ash and slag, as pozzolanic additions to partially replace Portland cement in the mixtures is a usual approach to reduce the cement content in concrete. This approach is, however, strongly dependent on the availability of by-products with qualified pozzolanic properties. Due to more strict environmental regulations, coal power plants are reducing, implying less and less availability of fly ash in the future. With the technical development of steel industry, the quality of slag may vary more and more.

Therefore, new and more sustainable approaches are needed for corrosion prevention or protection of reinforcement steel in concrete. Because concrete is porous and contains electrolytic pore solution, using the principle of electrochemistry in concrete is probably a more active way for corrosion prevention of reinforcement in concrete. In such way the properties of concrete with high water-cement ratio may better be utilized.

Electrochemical rehabilitation methods are commonly referred to cathodic protection (CP) and prevention (CPre), electrochemical realkalisation (ERA) and electrochemical chloride removal (ECR). Cathodic protection technique have great acceptance and well-established standards and guidelines in engineering applications. European standard *EN ISO 12696* and American standard "RP0290-90 Standard Recommended Practice - Cathodic Protection of Reinforcing Steel in Atmospherically Exposed Concrete Structures"

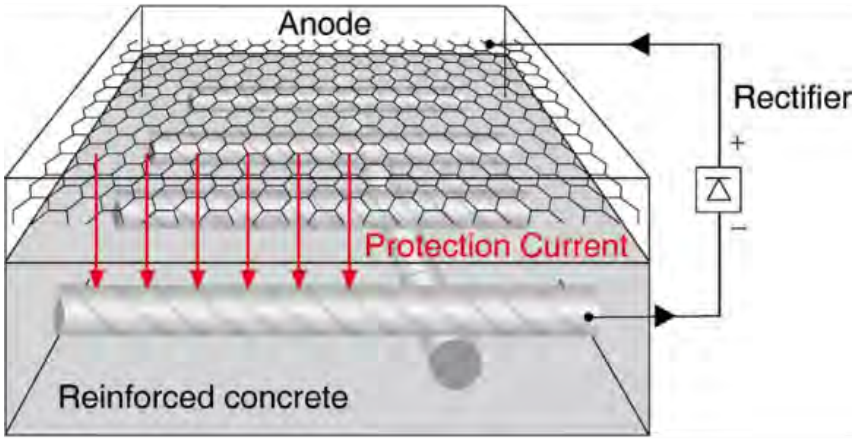

Figure 1.1: Schematic drawing of cathodic protection or cathodic prevention of reinforcement of concrete structures.

are available. ERA and ECR methods have also been studies (Miranda et al. 2006; Bastidas et al. 2008; Miranda et al. 2007), however, mainly on laboratory scales.

This work has been focused on cathodic protection and prevention method and accelerated test was designed as an analysis and evaluation tool of this approach.

1.2 Theoretical framework

Cathodic protection and prevention is now well-accepted as a powerful and efficient method for reducing corrosion rate and improve corrosion resistance of reinforcing steel in concrete (Bertolini et al. 1998). Impressed current cathodic protection (ICCP) is achieved by means of an anode system usually laid on the concrete surface and connected with the positive terminal of a direct voltage source; while reinforcement acting as cathode and connected with the negative terminal, as shown in Figure 1.1. By shifting the electrical potential negatively the reinforcements are forced into passivity or immunity state.

In some cases, cathodic protection measure is called "cathodic prevention", when it is applied on new structures that are expected to become contaminated by chloride during their service life. A small cathodic polarization of the steel should be applied on in the beginning of the service life. The current density for cathodic protection is 2-20 mA/m^2 (of steel surface) and for prevention it is 0.2-2 mA/m^2 (ISO-12696 2012). The principle of cathodic protection and prevention is illustrated in Figure 1.2 (Bertolini et al. 2009).

Conventional cathodic protection technique of steel reinforcement in concrete structures has been proved to be efficient and effective (Ahmad 2006; Pedeferri 1996). Many researchers have reported positive results based on case studies and practical experience (Polder 1998; Virmani and Clemena 1998; Schreyer 1997; Chadwich 1997). The electrochemical reactions occurred at cathode and anode depend on the environment, such the diffusivity of oxygen and exposure conditions. The primary reactions are, for example:

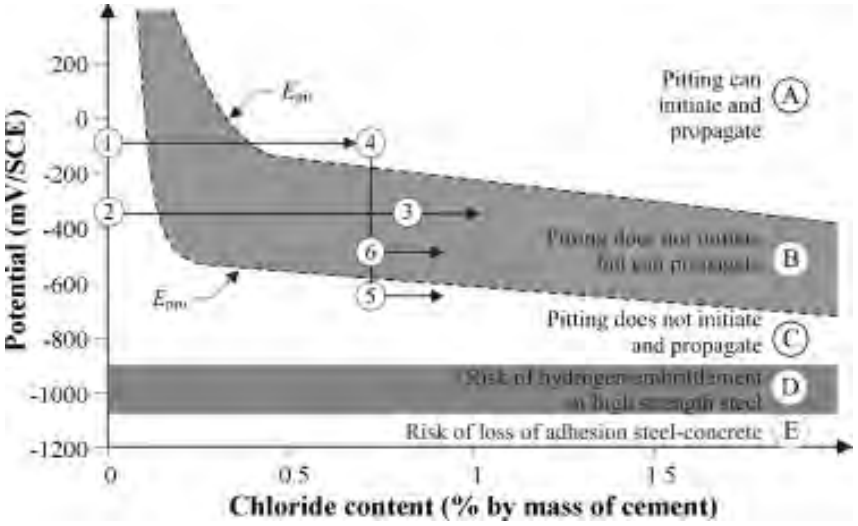

Figure 1.2: Schematic illustration of steel behavior in concrete as a function of the chloride content (Bertolini et al. 2009). Cathodic prevention (1→2→3); cathodic protection restoring passivity (1→4→6); cathodic protection reducing corrosion rate (1→4→5). Cathodic prevention is applied from the beginning at point 1; cathodic protection only after corrosion has initiated at point 4

- Primary reaction at the cathode (rebar): $O_2 + 2H_2O + 4e^- \rightarrow 4OH^-$;
- Primary reaction at the anode: $2H_2O \rightarrow O_2 + 4H^+ + 4e^-$;

  If in the presence of chlorides, chlorine develops: $2Cl^- \rightarrow Cl_2(\uparrow) + 2e^-$;

The beneficial effects of long-term cathodic protection can be concluded as three folds (Pedeferri 1996): (1) the corrosion rate is reduced or even can be negligible by taking the steel into passivity or immunity state; (2) increased alkalinity enables the steel to restore passivity because of the production of hydroxide ions (OH^-) at the steel surface; (3) the concentration of chloride ions (Cl^-) is decreased because of the migration of chloride ions moving away from the steel reinforcement (Eichler et al. 2010).

However, due to the nature of electrochemical reactions, cathodic protection may also present some side-effects, i.e. (1) hydrogen embrittlement due to overprotection which is sensitive to pre-stressed steel (Enos et al. 1997); (2) anode degradation or loss of adhesion between anode and concrete due to acid formation (Peelen et al. 2008); (3) risk of alkali-silica reaction in case of the presence of reactive aggregates due to higher concentration of OH^- in the pore solution (Sergi et al. 1991; Orellan et al. 2004). Besides the high costs of anode materials and complex monitoring system, the service life of cathodic protection system is not very satisfactory yet. The average service life of CP system is around 20 years and at the time of 15 years minor maintenance is usually required (Polder et al. 2014).

In order to improve conventional CP technique, many developments and innovative ideas have been invented and investigated. Cathodic prevention, using a low cathodic current density on new reinforced concrete structures, is designed to overcome the drawbacks of conventional CP system. Hydrogen embrittlement can be avoid so that CPre technique

can be safely applied also to pre-stressed steel reinforced structures (Bertolini et al. 1993; Bertolini et al. 1997). The chloride threshold value can be increased even by a very low current density of 0.4 mA/m^2 (Bertolini et al. 1998; Ahmad 2006). Based on these results, cathodic prevention technique is expected to have an extended field of applications and prolonged service life, which also brings benefits regarding economic costs and energy consumption. Many scientific articles and case studies have also described the successful operations of cathodic prevention even in the period of 10 years and suggested that cathodic prevention is a cost effective solution for reinforced concrete structures (Bertolini et al. 1997; Bazzoni et al. 2006; Chaudhary 2002; Tettamanti et al. 1997; Bazzoni et al. 1996).

Anode system as a key component in an ICCP system has great impact on the performance and durability of the system. Mixed-metal oxide titanium (MMO/Ti) anodes have gained great acceptance for CP applications for the high current capacity, light weight and low consumption rate (Heidersbach et al. 2006). However their extensive use was restricted due to their high costs (Dreyman 1972). Polymer composites anodes, especially carbon-polymer composites, as an attractive alternative have nowadays shown great potential as for its affordable costs, good electrical properties and versatility in manufacture. Carbon based material, as being considered the material of future technology, has drawn great attention and been under extensive study. Kessler and Powers (1989) have developed a type of conductive rubber anodes for steel reinforced concrete structures in marine environment, which contains ethylene-pylene-diene monomer (EPDM) and conductive carbon black. Graphite conductor embedded polymer anodes has been used for cathodic prevention application for coastal reinforced concrete structures (Heidersbach et al. 2006). Conductive coating overlay containing graphite or carbon fiber reinforced cement has been verified to be suitable to use in cathodic protection system (Jing and Wu 2011; Bertolini et al. 2004; Darowicki et al. 2003). Park and Park (2014) has reported that TiO_2 nanoparticles and graphene nanoplatelets can successfully be eletrophoretically co-deposited onto stainless steel and provide sufficient negative potential shift (from -0.4 V SCE to -0.7 V SCE) when exposed to UV light.

However investigations of carbon fiber reinforced composites as anode for CP/CPre system are relatively new (Mahdi 2010; Mayer 2004). Mork et al. (2006) found that carbon fiber net anode showed no loss of weight and no defects when the system was applied to polarization voltage up to 1.8 V and the protection current is 1-2 mA/m^2. Mahdi (2010) reported in his doctoral thesis that carbon fiber composite can be used as anode material in cathodic protection or prevention systems and the polarization potential should not be above 300 mV. Above this value the functioning life of the system might be estimated based on the weight loss of the carbon fiber net (Rob and Willy 2011). In a technical report, Mork et al. (2007) also monitored and investigated a harbor structure in Honningsvaag in Norway. The anode system consisted of carbon fiber meshes and cement based mortar and the CP system was achieved by a current density of 2 to 5 mA/m^2 and a voltage of maximum 1.8 V. The system was functioning well at the day of publishing according to European standard EN 12696.

Since studies of carbon fiber reinforced composites as anode material is rare, this work is designed to gain more knowledge on the specific application for cathodic prevention

system in reinforced concrete structures. The study of impact on microstructures and preliminary method of service life prediction have been highlighted. The conclusions and recommendations for future work have been underlined as well.

1.3 Objectives and limitations

The overall objective of this work is to investigate the effect caused by current exchange on macro- and micro-structures of reinforced concrete structures and to evaluate the feasibility of applying carbon fiber mesh as anode material for a long-term cathodic prevention system in reinforced concrete structures when exposed to chlorides. To achieve the general aim, three specific objectives of research has been studied:

1. To analysis of chemical and microstructure changes at the anode (carbon fiber mesh) zone after accelerated electrochemical treatment;
2. To study of the mechanism of possible degradation processes under the long-term cathodic protection/prevention; and
3. To develop applicable models and tools for service life design.

The experimental work was focused on paste and mortar materials for electrochemical accelerated method in favor of further microstructure analysis. The purpose of paste groups is to investigate chemical compositions and microstructures before and after the acceleration tests, whilst for mortar groups the aim is to evaluate the long-term durability of this innovative anode material and the system by monitoring the material damage and estimating the equivalent service life of the system. In this work, all the specimens are considered submerged or exposed in the tidal zone. Carbonation is not taken into consideration. Concrete material is not included in this study due to the limited period of time. The general assumption of this work was that 2 mA/m^2 could sufficiently provide protection according to *EN ISO 12696*, which is the principle for estimation of the equivalent service life. Moreover, the degree of surface damage and acceleration time was assumed to be in linear relation.

Chapter 2

Overview of experimental program

In order to perform long-term (100 years) cathodic prevention analysis, an accelerated test method must be developed to shorten the experimental time. Conventional experimental method using low current density (1-2 mA/m^2) is impossible to carry out since the time range is too long. Therefore in the accelerated test the current density was increased for this purpose.

The concept of accelerated tests was to increase the current density applied into the system in order to shorten the total testing period into a manageable length. The total amount of electrons applied into the system was defined as a polarization parameter Φ (Chang 2002).

$$\Phi = I_a \times t_a \tag{2.1}$$

where Φ is the total amount of electrical charge applied to the system during the entire period of acceleration test. [C/m^2, where C is abbreviation for Coulomb];
I_a, the applied current density into the system [A/m^2];
t_a, the duration that the applied current density is available [s];

To estimate the service life of anode system by using electrochemical acceleration method, the general principle is as following:

$$I_a \times t_a = I_e \times t_e \tag{2.2}$$

where Φ is the same as in Equation 2.1, but the unit can be expressed as [$mA \cdot m^{-2} \cdot days$] for convenience in engineering practice;
I_a, the accelerated current density, which is equal to "current density of wet steel (mA/m^2)" as shown in Table 3.3 and Table 3.4 [mA/m^2];
t_a, the accelerated testing period;
I_e, typical current density of cathodic prevention (0.2-2.0 mA/m^2), where in this test the upper limit 2.0 mA/m^2 is chosen for estimation the service life in real case [mA/m^2];
t_e, the estimated equivalent service life of cathodic prevention system in real case [days].

Table 2.1: Description of the testing program

	Paste specimens	Mortar specimens
Exposure condition	Partially submerged in 10% NaCl solution	Partially submerged in 10% NaCl solution
Specimen	Two groups of specimens coded as ACC-P1 and ACC-P2	Two groups of specimens coded as ACC-M1 and ACC-M2
Experimental purpose	Designed to investigate chemical and microstructure properties	Designed to examine the equivalent service life

So that the equivalent time t_e at a typical current density for cathodic prevention can be rearranged as:

$$t_e = \frac{I_a}{I_e} \times t_a \tag{2.3}$$

For example, when the polarization parameter Φ is 2000 [mA·m^{-2}·days], if a cathodic prevention current 2 mA/m^2 is used as in engineering practice, then the predicted service life is 1000 days (2.7 years). It is worth mentioning that the estimated equivalent time is on the conservative side, because extra damage may be caused by using accelerated test method.

The testing program were divided mainly into two parts, depending on the mix design, as shown in Table 2.1. In each category, the main experimental parameters are: (i) applied current density and (ii) the length of test period; while the safety and efficiency of electrical set-up and protection of specimens from unexpected damage have to be considered.

Chapter 3

Accelerated test of paste specimens

This chapter describes the experimental details of paste group ACC-P1 and ACC-P2.

3.1 Materials

The material used for paste specimens were:

- Swedish structural cement (Slite Anläggninscement) with a w/c ratio of 0.6;
- Steel reinforcement (plain bars) with a diameter of 10 mm;
- Titanium oxides anode mesh (ELGARDTM 210 CORRPRO®) used in one specimen as comparison;
- Carbon fiber reinforced polymer (CFRP) mesh as anode as shown in Figure 3.1 (SIGRATEX Grid 300 supplied by SGL Group) with inner spacing of 25 mm × 25 mm, containing two fiber threads in both vertical and horizontal directions. Each fiber thread was about 2-3 mm in width.

Figure 3.1: Carbon fiber mesh (SIGRATEX Grid 300) as anode material

Table 3.1: Surface area of steel reinforcement of paste group ACC-P1

Description	Parameter	Value	Unit
Length of total steel in specimen	L_{tot}	250	mm
Length of immersed steel in solution	$L_{steel\ in\ solution}$	200	mm
Diameter of smooth steel bar	ϕ_{steel}	10	mm
Surface area of immersed steel bar	$A_{wet\ surface}$	6.28×10^{-3}	m^2
Surface area of total steel bar	A_{total}	7.85×10^{-3}	m^2

Table 3.2: Surface area of steel reinforcement of paste group ACC-P2

Description	Parameter	Value	Unit
Length of total steel in specimen	L_{tot}	160	mm
Length of immersed steel in solution	$L_{steel\ in\ solution}$	130	mm
Diameter of smooth steel bar	ϕ_{steel}	10	mm
Surface area of immersed steel bar	$A_{wet\ surface}$	4.08×10^{-3}	m^2
Surface area of total steel bar	A_{total}	5.02×10^{-3}	m^2

3.2 Dimension of paste specimens

The dimension of specimen group ACC-P1 was 40 mm × 40 mm × 250 mm as illustrated in Figure 3.2. The bottom of the specimen were protected by epoxy resin coating. Each specimen was immersed in 10% NaCl solution with the solution level at 200 mm position from the bottom. The surface areas of steel reinforcements are shown in Table 3.1.

The dimension of specimen group ACC-P2 was 40 mm × 40 mm × 160 mm as illustrated in Figure 3.3. All the surfaces except the one for exposure were covered by epoxy resin coating. Each specimen was immersed in 10% NaCl solution with the solution level at 130 mm position from the bottom. The surface areas of steel reinforcements are shown in Table 3.2.

3.3 Experiment set-up for accelerated test

Specimen group ACC-P1 contained 6 specimens and they were connected to different currents. All specimens were partially submerged in a 10% sodium chloride (NaCl) solution. The reinforced steel bars were connected to the negative terminal of the external power supply acting as cathode and the carbon fiber mesh anode to the positive terminal. Figure 3.4 shows the experiment set-up and the appearance of the specimens before and after the accelerated test.

Figure 3.5 shows the experiment set-up of paste group ACC-P2. Specimen group ACC-P2

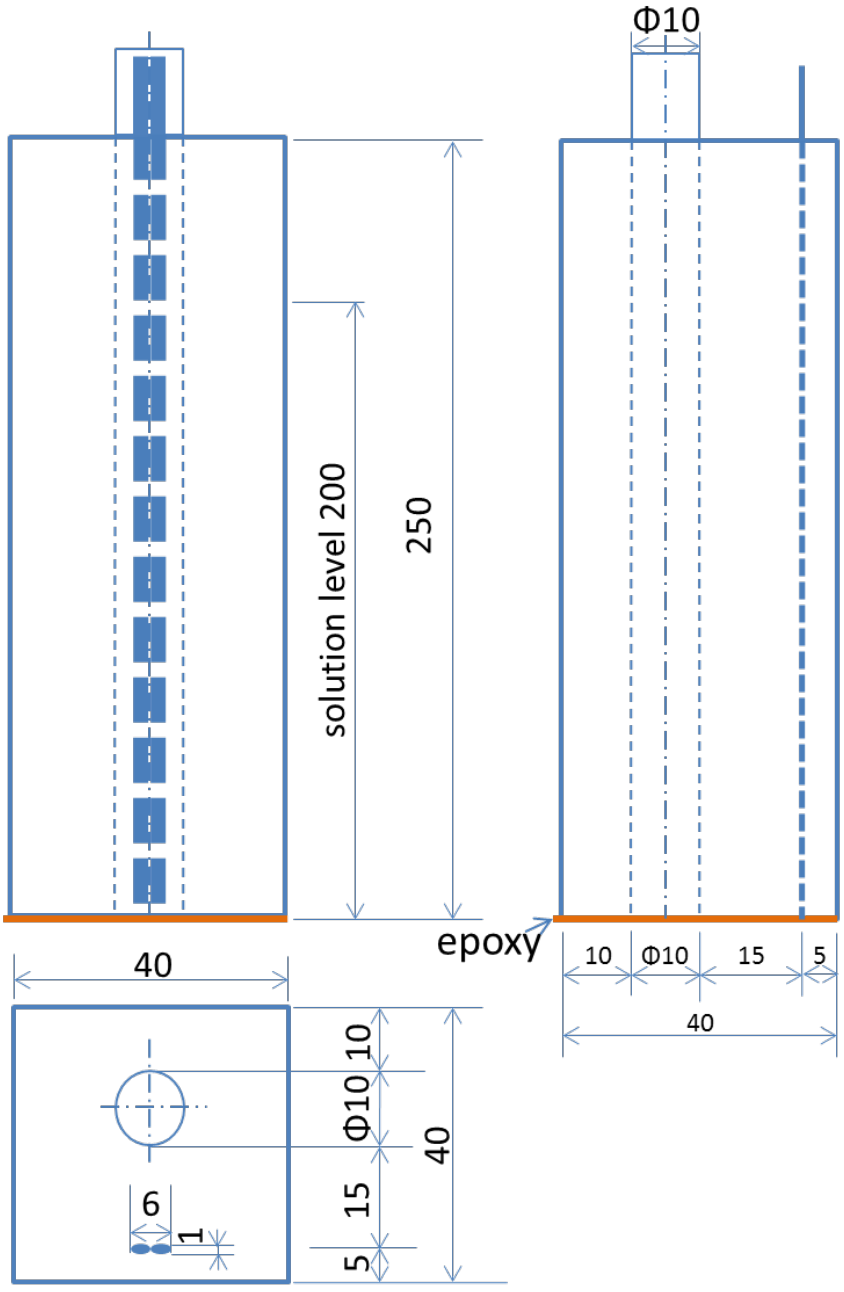

Figure 3.2: Three-view drawing of specimen group ACC-P1

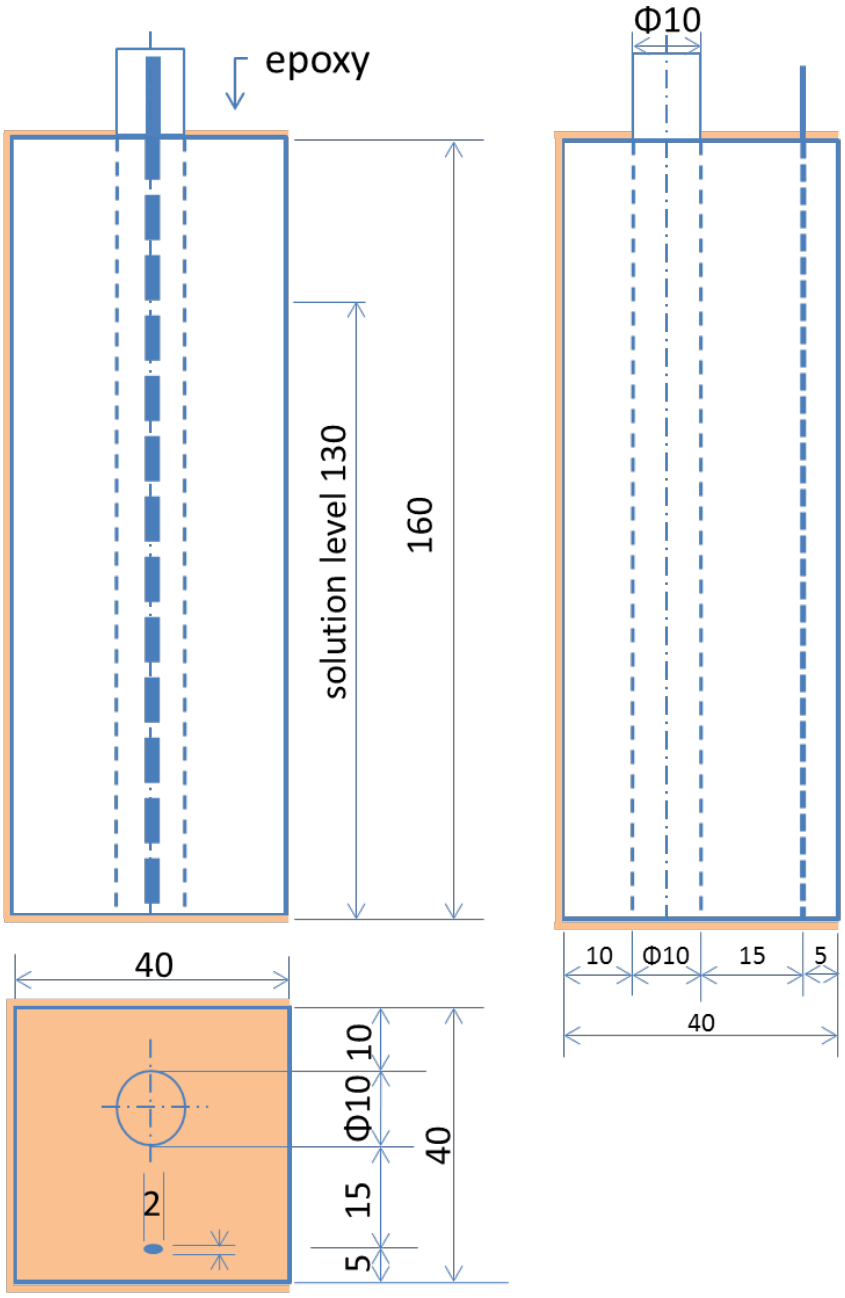

Figure 3.3: Three-view drawing of specimen ACC-P2

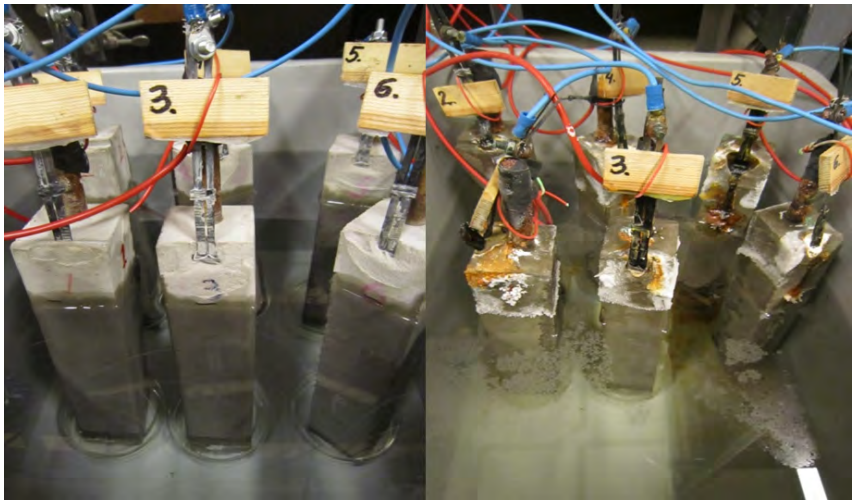

Figure 3.4: Group ACC-P1 specimens before (left) and after (right) the accelerated test

Figure 3.5: Group ACC-P2 specimens before the accelerated test

contained 6 specimens, which were connected to different currents in separate solutions, and one control specimen as reference, which was not connected to power supply. Titanium oxides metal was used as anode in specimen number 5 (P2-5) and the rest of specimen contained carbon fiber as anode. Each specimen was individually submerged in a 10% NaCl solution. The reinforced steel bars were connected to the negative terminal of the external power supply acting as cathode and the carbon fiber mesh anode to the positive terminal.

3.4 Applied current density for paste specimens

For specimen group ACC-P1, the applied current density and estimated service life are listed in Table 3.3. For specimen group ACC-P2, the applied current density is listed in Table 3.4. Titanium oxide metal was used as anode in sample number 5 (P2-5), instead of carbon fiber mesh .

Table 3.3: Details of accelerated tests of group ACC-P1

Specimen number	P1-1	P1-2	AP1-3	P1-4	P1-5	P1-6
Binder type			OPC w/c=0.6			
Testing period [days]			60			
Applied current [mA]	25	19	13	6	5	4
Current density [mA/m^2]	5000	4000	3000	2000	1000	800
Absolute Coulomb value [C]	130222	97667	65111	32556	26044	19533
Equivalent service life [days]	240000	180000	120000	60000	48000	36000
Equivalent service life [years]	658	493	329	164	132	99

Table 3.4: Details of accelerated tests of group ACC-P2

Specimen number	P2-1	P2-2	P2-3	P2-4	P2-5	P2-6
Binder type			OPC w/c=0.6			
Testing period [days]			60			
Applied current [mA]	4	25	19	13	6	5
Current density [mA/m^2]	923	6154	4615	3077	1538	1231
Absolute Coulomb value [C]	20736	130222	97667	65111	32556	26044
Equivalent service life [days]	27692	184615	138462	92308	46154	36923
Equivalent service life [years]	76	487	360	234	123	97

Chapter 4

Accelerated test of mortar specimens

This chapter describes the experimental details of mortar group ACC-M1 and ACC-M2.

4.1 Materials

The raw materials used for mortar specimen were:

- Swedish structural cement (Slite Anläggninscement) with a water/binder ratio (w/b) of 0.6;
- Fly ash (FA), manufactured by Noecem AS (Norway);
- Ground granulated blast-furnace slag (GGBS), commercially available as Merit 5000, supplied by Merox (Sweden);
- CFRP mesh as anode (SIGRATEX Grid 300 supplied by SGL Group);
- Steel reinforcement (plain bars) with a diameter of 10 mm.

The mix design of mortar is given in Table 4.1.

4.2 Dimension of mortar specimens

The dimension of specimen group ACC-M1 and ACC-M2 was 300 mm × 200 mm × 50 mm and each specimen was immersed in 10% NaCl solution with the solution level at 250 mm position from the bottom, as shown in Figure 4.1. The surface areas of steel reinforcements are shown in Table 4.2.

Table 4.1: Proportioning of mortar specimens

Binder system	OPC	PC+20%FA	PC+25%GGBS
Group name	A	B	C
w/b ratio	0.6	0.6	0.6
Cement content (kg/m^3)	500	460	430
Sand content (0-4 mm) (kg/m^3)	1500	1500	1500
Water content (kg/m^3)	300	300	300
FA content (kg/m^3)	–	90	–
GGBS content (kg/m^3)	–	–	110
Water curing for test specimen (days)	7	7	7
Water curing for prism (days)	25	25	25

Table 4.2: Surface area of steel reinforcement of mortar groups ACC-M1 and ACC-M2

Description	Parameter	Value	Unit
Solution level of specimen	$L_{specimen\ in\ solution}$	250	mm
Length of total steel in specimen	L_{tot}	350	mm
Length of immersed steel in solution	$L_{steel\ in\ solution}$	200	mm
Diameter of smooth steel bar	ϕ_{steel}	10	mm
Surface area of immersed steel bar (2 bars)	$A_{wet\ surface}$	1.26×10^{-2}	m^2
Surface area of total steel bar (2 bars)	A_{total}	2.20×10^{-3}	m^2

4.3 Experiment set-up for accelerated test

Group ACC-M1 contained 6 specimens and group ACC-M2 contained 5 specimens. All specimens were partially submerged in 10% NaCl solutions. The same experimental set-up was used for both groups ACC-M1 and ACC-M2 as shown in Figure 4.2. The reinforced steel bars were connected to the negative terminal of the external power supply acting as cathode and the carbon fiber mesh anode to the positive terminal.

4.4 Applied current density for mortar specimens

Table 4.3 shows the applied current density and estimated service life of specimen group ACC-M1. The constant applied current for all specimens was 60 mA. The applied current density and estimated service life of specimen group ACC-M2, are given in Table 4.4. The constant applied current was 40 mA.

The testing purposes and procedures for ACC-M1 and ACC-M2 were different. For group ACC-M1, the anode-mortar interface and surface condition was monitored under the entire

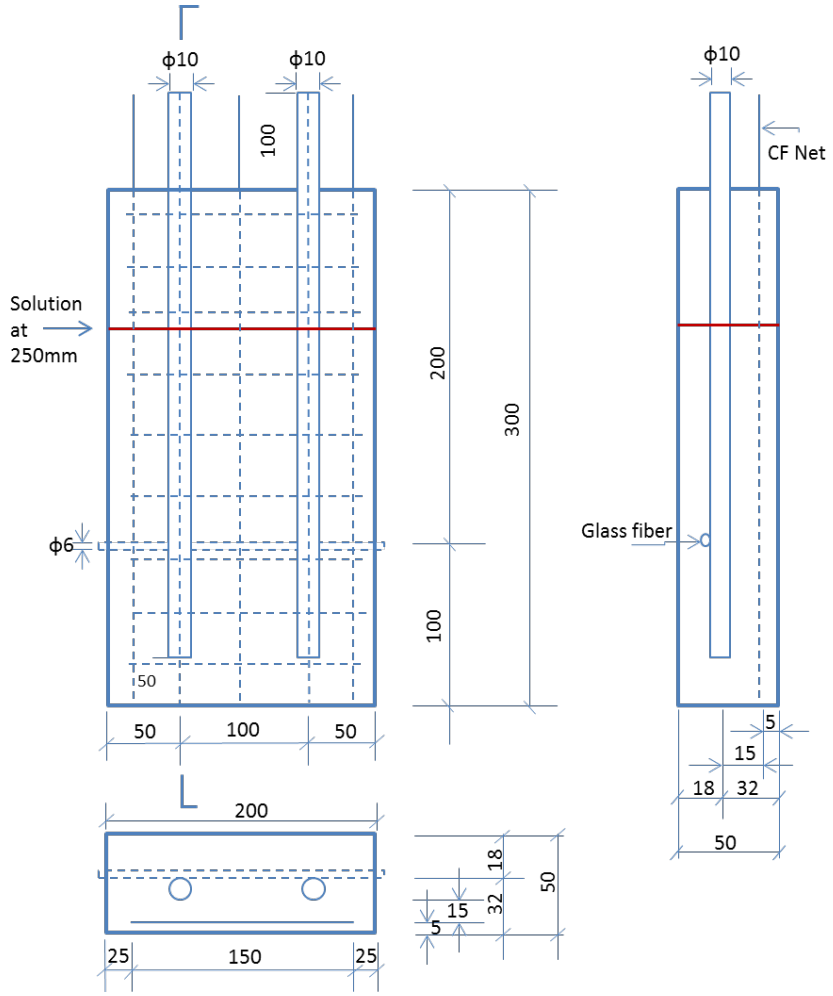

Figure 4.1: Three-viewing drawing of mortar specimen group ACC-M1 and ACC-M2.

Figure 4.2: Experiment set-up for group ACC-M2

Table 4.3: Applied current density and estimated service life of specimen group ACC-M1

Description	Value
Applied constant current (mA)	60
Current density of wet steel (mA/m^2)	4777
Acceleration time (days)	30
Equivalent service life t_e (days)	71656
Equivalent service life t_e (years)	196
Acceleration time (days)	60
Equivalent service life t_e (days)	143312
Equivalent service life t_e (years)	393

Table 4.4: Applied current density of specimen group ACC-M2

Description	Value
Applied constant current (mA)	40
Current density of wet steel (mA/m^2)	3185

designed test period (30 days and 60 days); while for group ACC-M2, acceleration time was recorded until a damage occurred on the specimen or the ICCP system was failed. The criteria for determining the end point for acceleration test were presented in Section 6.4.

Chapter 5

Analytical methods

5.1 LA-ICP-MS

Laser ablation-inductively coupled plasma-mass spectroscopy quantified the longitudinal changes in the distribution of elements. A schematic diagram of LA-ICP-MS instrument is shown in Figure 5.1. The chemical analysis of treated specimen was carried out by Laser Ablation analysis at University of Gothenburg, using a New Wave NWR213 laser ablation system coupled to an Agilent 7500a quadrupole ICP-MS.

A Large Format Cell holds samples up to 10 cm $\times$ 10 cm in size, combined with a 1 cm diameter ablation chamber at the ablation region, enabling fast washout anywhere in the sample chamber. A 30 μm laser spot size, beam energy density of about 6 J/cm^2 and repetition rate of 10 Hz was used in line scan mode, with a scan speed of 60 or 100 μm/s. The sample and ablation chamber were flushed with helium to carry the aerosol produced during ablation to the ICP-MS. Before reaching the torch, the carrier gas was mixed with argon and nitrogen, with total flow rates around 0.90 l/min helium, 0.65 l/min argon and 5 ml/min nitrogen.

Each measurement consisted of 30 s background followed by 100 s -200 s of signal collection. Dwell times are 10 ms for masses analyzed, which included ^{13}C, ^{23}Na, ^{24}Mg, ^{27}Al, ^{28}Si or ^{29}Si, ^{34}S, ^{35}Cl, ^{39}K, ^{43}Ca, ^{47}Ti, ^{55}Mn and ^{57}Fe. Quantification was performed by frequently measuring the glass standard SRM NIST 610 using values by Jochum et al. (2011). Variations in calculated abundances of all measured isotopes, except for C, S and Cl, which are too low to be quantified in SRM NIST 610, was less than 10% throughout a whole analytical session.

5.2 SEM

The chemical composition and surface image analysis was carried out at Gothenburg University by a Hitachi S-3400N Variable Pressure SEM integrated with energy-dispersive

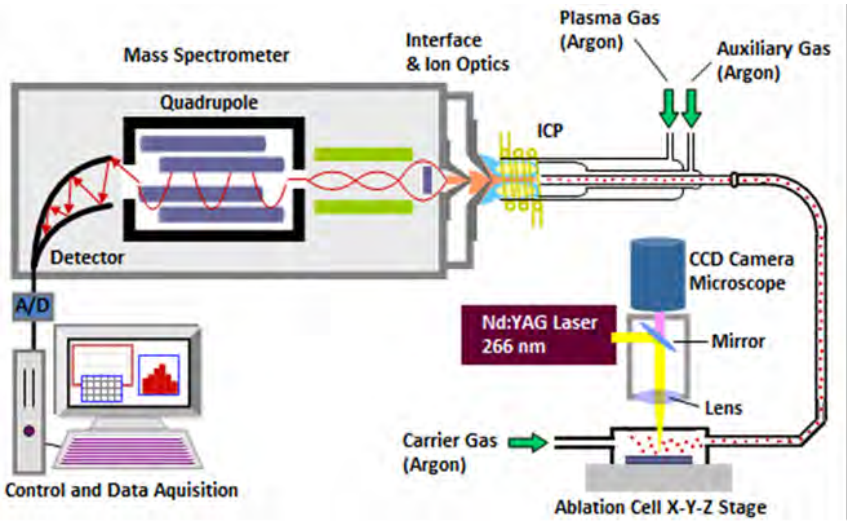

Figure 5.1: A schematic diagram of LA-ICP-MS technique (Silva et al. 2013)

Figure 5.2: Hitachi S-3400N Variable Pressure SEM with EDS spectrometer

spectrometer (EDS). Accelerating voltage was 20kV. Detection limits were about 0.1% with EDS (1000 ppm). Backscattered electron (BSE) mode was used to examine cement paste samples. A picture of Hitachi SEM instrument is shown in Figure 5.2.

Chapter 6

Results and discussions

6.1 Microstructure study on control samples

A carbon fiber thread from mesh embedded in cement paste without any electrochemical acceleration treatment was used a control sample to investigate the chemical composition without the effect from external electrical field. The control sample was also partially submerged in a 10% NaCl solution.

A SEM image of control sample is shown in Figure 6.2. The dimension of a carbon fiber thread at the widest and longest point were about 3 mm and 0.6 mm, respectively. The semi-quantitative analysis of chemical composition of control sample by LA-ICP-MS is listed in Table 6.1, as a baseline of specimens without electrochemical treatment. For the analysis result of each element, the data were presented in the Appendix. Figure 6.1 shows the calcium silica mole ratio (Ca/Si) of the control sample was around 3.

In comparison with the chemical analysis of clinker composition (provided by the manufacturer CEMENTA), the high concentration of sodium and chloride were due to the diffusion of ions from the immersion solution, so that the results of sodium and chloride were not comparable with the clinker composition.

6.2 Ring-pattern around anode

After two-month period of connection to external electrical field, the specimen was taken out, sawed into slice and the dimension of the ring-pattern around carbon fiber anode was investigated, as shown in Figure 6.3. Figure 6.4 shows a back-scattered SEM image that confirmed the layered ring-pattern area with different phases. The dimension of the affected zone was from 0.5 to 2 mm around the anode.

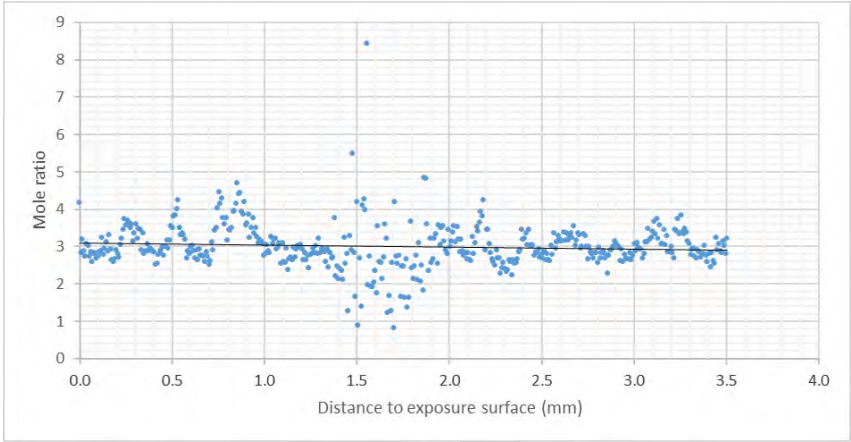

Figure 6.1: Ca/Si mole ratio is around 3 in control sample. At distance between 1.5 to 2 mm is the location of carbon fiber anode.

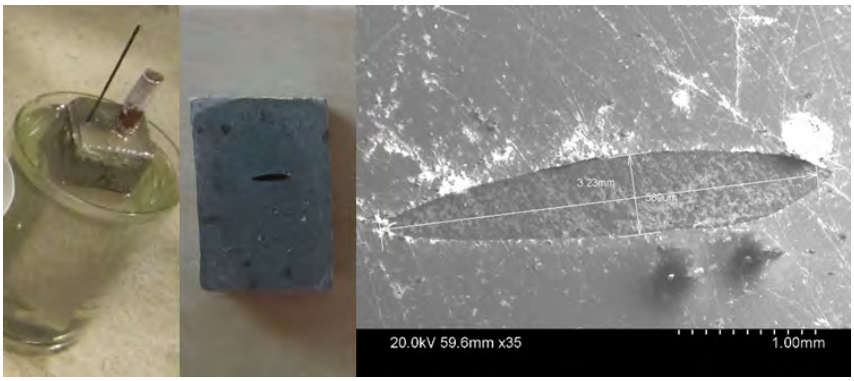

Figure 6.2: SEM image of the cross section of the control sample and dimension of a carbon fiber thread

Table 6.1: LA-ICP-MS chemical analysis of control sample compared with clinker composition provided by the manufacturer

Composition	Clinker (wt%)	LA-ICP-MS analysis (wt%)
CaO	64.1	64
SiO_2	22.5	24
Al_2O_3	3.1	3.5
Fe_2O_3	4.0	3.0
MgO	1.3	1.1
Na_2O	0.12	2.2
K_2O	0.58	0.3
SO_3	2.6	–
Cl	0.01	3.4

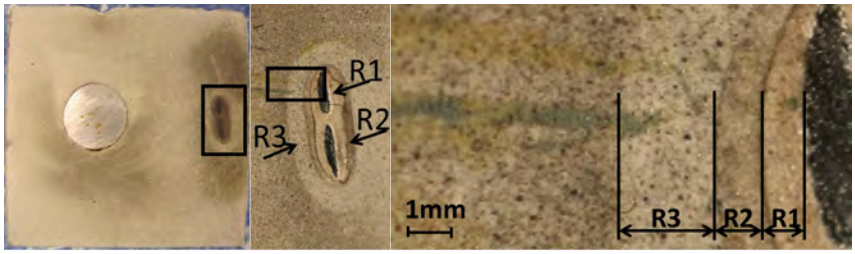

Figure 6.3: Sawed samples (left), ring-pattern (middle) and the dimension of the ring-pattern (right). Dimension of the ring-pattern is around 1mm to 2 mm (from specimen ACC-P1-5, equivalent service life is 132 years)

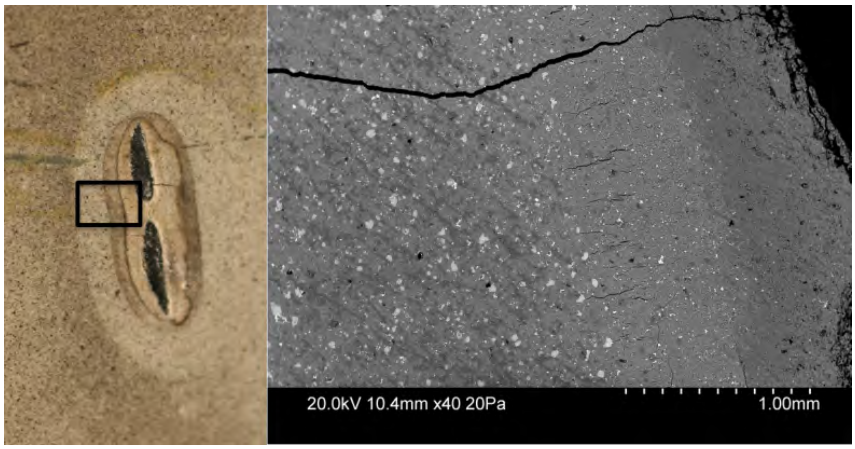

Figure 6.4: Back-scattered SEM image of the ring-pattern area, shown different phases of the ring-pattern area around anode. The crack through the ring area was formed after experiment, caused by drying (from specimen ACC-P1-5, equivalent service life 132 years)

6.3 Compositional changes at anode zone

A change in the Ca/Si ratio in the vicinity of anode was observed by both the SEM and LA-ICP-MS measurements. Table 6.2 presents the Ca/Si ratio in the zone close to anode compared with the Ca/Si ratio in paste matrix. The results showed a trend of decrease in the Ca/Si ratio from Ring-3 (representing the sound zone) to Ring-1 (representing the affected zone), while Na/Si ratio was increased. The same trend was observed by measuring the concentration of each element using LA-ICP-MS, as shown in Figure 6.6. Results showed that at the area close to the carbon fiber anode, the concentration of Ca was lower than that in the cementitious matrix. This phenomenon is because that the ion migration under the feeding potential, under which the positive Ca^{2+} in the pore solution (disolved from Portlandite, $Ca(OH)_2$) has been migrated away from the anode.

Due to the nature of C-S-H gel, the distribution of silicon in the cement paste matrix has been assumed unchanged because the Si–O bonding is very stable and hardly to be broken or reformed even under strong acid environment at a high temperature (Ryu et al. 2002). Therefore the changes of Ca/Si ratio were considered as the changes of calcium in the cement paste matrix.

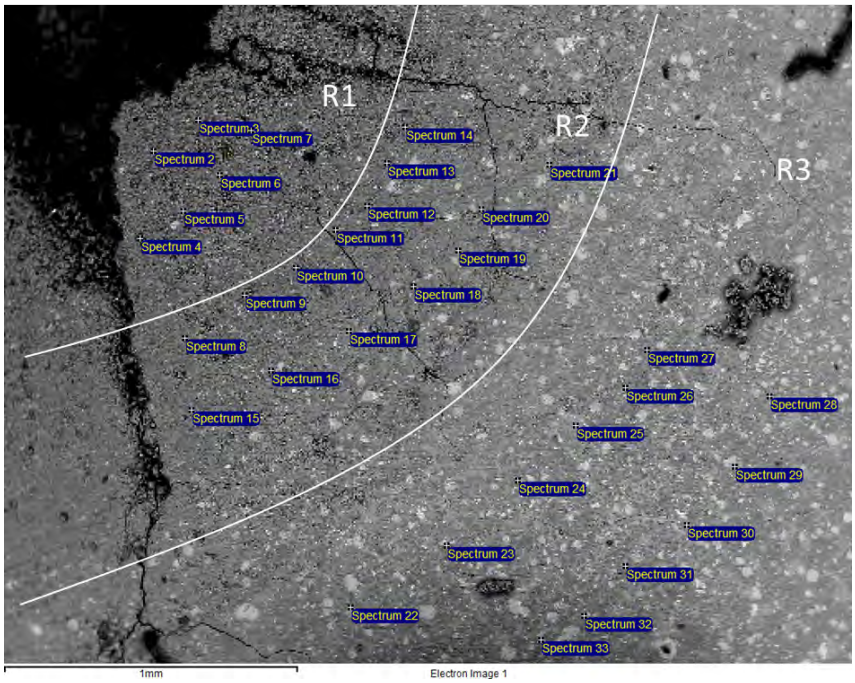

Figure 6.5: Spot analysis of specimen ACC-P2-5, which the service life is equivalent to 123 year

Table 6.2: Calcium and sodium content at each leached zone around the anode

Leached zone	Ca/Si ratio	Na/Si ratio
Ring-1	2.63	0.20
Ring-2	3.50	0.11
Ring-3	5.88	0.07

On the other hand, positive ions sodium (Na^+) did not show the same movement as calcium. In Figure 6.6, the molar concentration of sodium reached a peak and then gradually decreased to a base level. The possible explanation might be as follows. Under the electrochemical treatment the hydrogen ions were formed around the anode from the electrolysis of water. These hydrogen ions (H^+) produced locally acidic condition which dissolved Portlandite. The dissolved calcium ions moved away from the zone around the anode, forming rings with lower ratios of Ca/Si, as discussed above. After termination of the electrochemical treatment, sodium ions, which have significantly higher diffusivity than that of calcium ions, diffused from the surrounding cement paste matrix back to the zones around the anode to substitute the negatively charged sites of C-S-H gel previously occupied by the calcium ions to keep the electroneutrality, resulting in peaks of Na/Si around the anode.

SEM analysis also found NaCl crystals at the anode and in the ring-pattern affected zone. In Figure 6.7, the white substances (left) were confirmed as NaCl crystals (right).

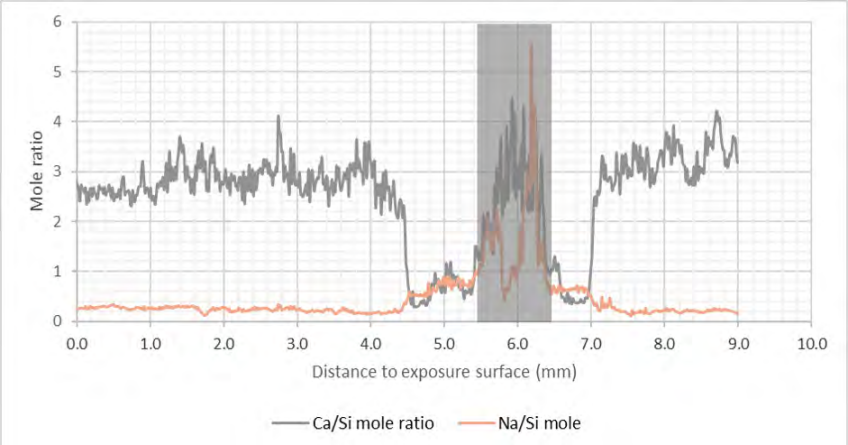

Figure 6.6: [ACC-P2-3, 360 years of equivalent service life] Line scanning by LA-ICP-MS across the cross-section of accelerated specimen. The shadowed area indicates the position of carbon fiber

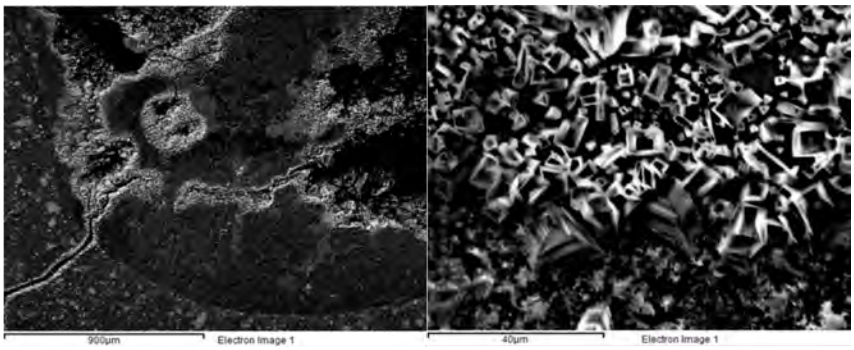

Figure 6.7: [ACC-P2-3, 360 years of equivalent service life] NaCl crystals at anode and ring-pattern affected zone

LA-ICP-MS analysis has detected high concentration of NaCl in the anode area but not in the ring-pattern effected area, as shown in Figure 6.8, compared with the baselines of Na/Si and Cl/Si in Figure 6.9). This is probably due to sample preparation of SEM analysis. After careful surface polishing, substances in the ring-pattern affected zone and the anode area could move around because they are relatively loose; while sample polishing for LA-ICP-MS was very brief and fast.

Precipitation of NaCl at the anode can be considered as a preventative effect of hindering chloride further migrating towards steel reinforcement. However higher concentration of chloride might promote the production of chlorine gas which has potential risk of inducing internal cracks and hazard issue.

6.4 Surface condition of mortar specimens

The current density used for group ACC-M1 was about 5 A/m^2 (see Table 4.3), which was much higher than typical prevention current density normally in the range of 0.2 to 2

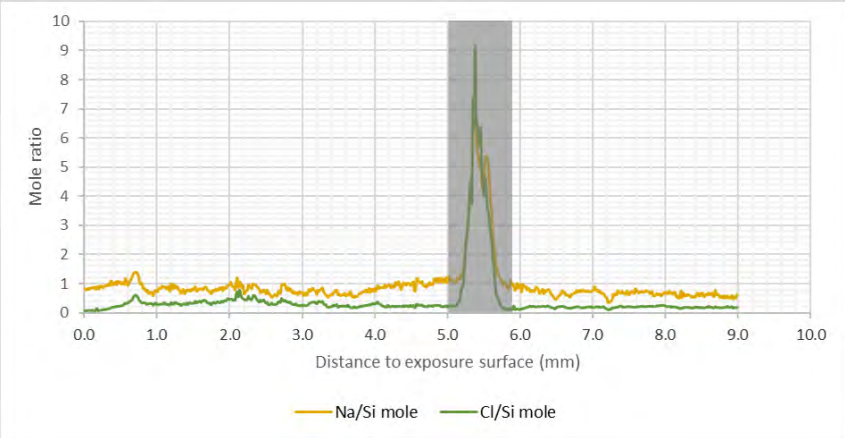

Figure 6.8: [ACC-P2-3, 360 years of equivalent service life] High concentration of Na and Cl at anode area. The shadowed area indicates the position of CFRP anode

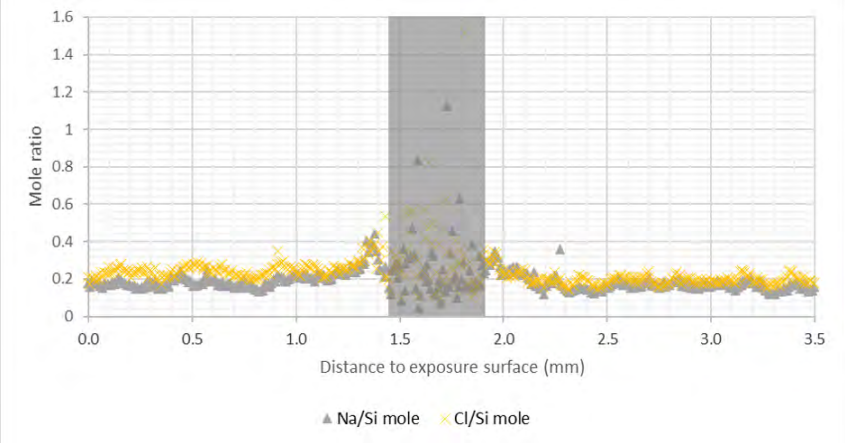

Figure 6.9: Concentration of Na and Cl of the control sample. The shadowed area indicates the position of carbon fiber

mA/m^2. So here it is worth to point out again that the surface damage in the accelerated test should be worse than that under typical prevention current density. In other word, if the same level of surface damage would be reached under normal prevention current densities, the time it took should be longer than the estimated equivalent service life.

Figure 6.10 shows the surface damage after 30 days acceleration test (equivalent to 196 years). The surface damage was observed on specimens A (OPC) and C (PC+25%GGBS) at the position below and along the immersion line, whilst specimen B (PC+20%FA) still revealed a good surface condition, indicating that fly ash additive has better homogeneity than slag. Figure 6.11 shows the specimen with the same mix after 60 days acceleration test (equivalent to 393 years). All three specimens had surface damage along the immersion line, which indicated the area around immersion solution, as in real case as the tidal zone, can be considered as a critical area because it has higher risk of damage.

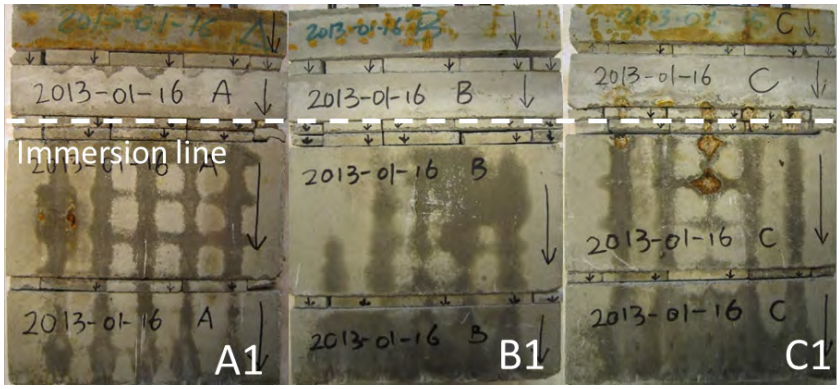

Figure 6.10: Group ACC-M1 specimen A1 to C1 after accelerated test. The detailed mix design is listed in Table 5. Specimen A – OPC; B – PC+20%FA; C – PC+25%GGBS. Designed equivalent service life is 196 years (see Table 4.3).

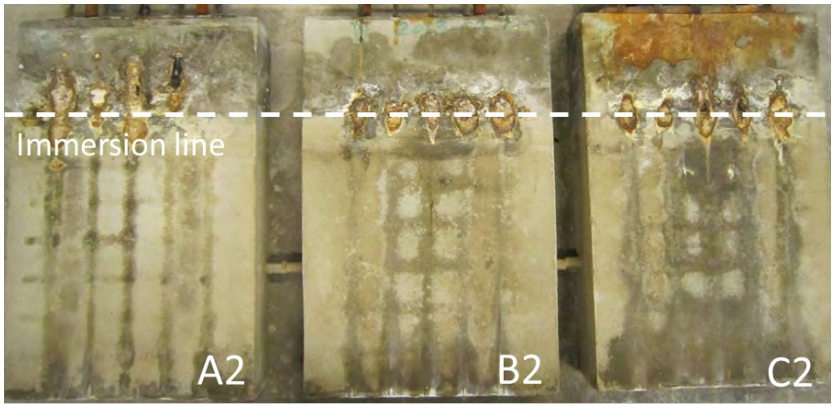

Figure 6.11: Group ACC-M1 specimen A2 to C2 after accelerated test. The detailed mix design is listed in Table 5. Specimen A – OPC; B – PC+20%FA; C – PC+25%GGBS. Designed equivalent service life is 393 years (see Table 4.3).

6.5 Equivalent service life of mortar specimens

For group ACC-M2, the applied current density was about 3 A/m^2 (see Table 6.3) for specimen OPC, FA and GGBS-1. For specimen GGBS-2 and GGBS-3, the current densities were reduced by 50% and 25%, respectively.

Two criteria were used to determine the end point of each specimen. One criterion was based on the appearance of the surface condition, that was, the experiment was terminated when the apparent surface damage was observed, e.g. specimens OPC, GGBS-1 to GGBS-3, as shown in Figure 6.12. Another criterion was dependent on the actual applied current, when there was no apparent surface damage observed. As in this case of specimen FA in Figure 6.12b, the experiment was terminated when the actual applied current density was lowered by 40% of the original value, indicating possible internal damage or disconnection due to the dramatic decrease in ionic concentration near the anode.

As for the damage location, specimen GGBS-2 and GGBS-3 showed the surface damage

Table 6.3: Estimated equivalent service life of mortar group ACC-M2

Specimen name	OPC	FA	GGBS-1	GGBS-2	GGBS-3
Applied current [mA]	40	40	40	20	10
Current density [mA/m^2]	3185	3185	3185	1592	796
Testing duration [days]	27[a]	68[b]	33[a]	82[a]	65[a]
Absolute coulomb value [C]	109058	224609	109001	144176	58743
Equivalent service life [days]	42994	108280	52548	65287	25876
Equivalent service life [years]	118	297	144	179	71

[a]Terminated due to apparent surface damage
[b]Terminated due to low prevention current densit

along the immersion line, which were in agreement with ACC-M1 specimen A2, B2 and C2. However, specimen OPC and GGBS-1 had damage below the immersion line, probably due to the inhomogeneity of the mortar material, or defects such as air bubble, micro-cracks and so on. Those internal defects or inhomogeneity can lead to locally higher current density, causing earlier damage in the defected area.

Among specimens GGBS-1 to GGBS-3, the service life were expected to be increased as the current density was lowered. Specimen GGBS-2 showed this trend but not specimen GGBS-3. Since the number of specimens was limited in this work, it was hard to conclude the relation between prolonged service life and lowered current density in this case. However, the trend was promising. As mentioned before, the inhomogeneity of microstructure could play an important role.

It is worth pointing out that the surface damage only gives a poor aesthetic appearance, without jeopardizing structural properties of the reinforced concrete, because the reinforcement steel is still prevented from corrosion as long as enough cathodic polarization current is imposed.

(a) OPC:Equiv. 118 yrs (27 days)

(b) FA:Equiv. 297 yrs (68 days)

(c) GGBS-1: Equiv.144 yrs (33 days)

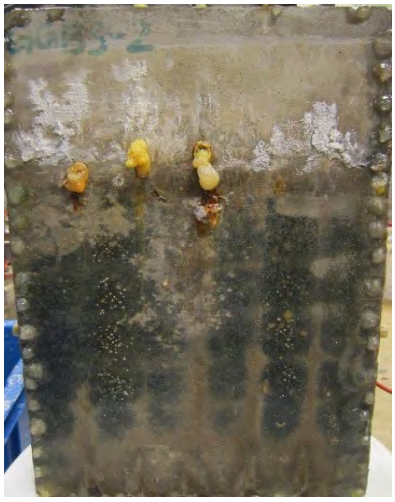

(d) GGBS-2: Equiv.179 yrs (82 days)

(e) GGBS-3: Equiv.71 yrs (65 days)

Figure 6.12: Mortar specimens after acceleration test

(a) Equiv. 96 yrs (22day) (b) Equiv. 118 yrs (27day) (c) Equiv. 127 yrs (29day)

Figure 6.13: OPC specimen at different acceleration stage

Chapter 7

Conclusions

This work was aimed to investigate the effect of accelerated current on macro- and microstructure of cementitious material and evaluate carbon fiber reinforced polymer mesh as anode material for long-term cathodic prevention system. Through the review of previous studies, it is safe to say that carbon fiber is an innovative material that attracts interests in many research topics regarding building materials and also shows a potential of many future applications in the area of civil engineering with the requirement of sustainable development. With the effort of this work, some general conclusions can be drawn as follows:

- Carbon fiber mesh was suitable for the application of cathodic prevention system for steel reinforced structures;
- The estimated equivalent service life were in general over 100 years;
- Electrochemical accelerated test can be used as a valuable tool to evaluate specimens in a short-term equivalent to a long-term exposure and to estimate the service life conservatively;
- The electrochemically affected zone around anode was found between 0.5 mm to 2 mm in diameter around the anode due to acidification and ion migration;
- Microstructural and chemical changes occurred at the anode-paste interface under a high current density. The carbon fiber after the accelerated test remained continuous shape by visual inspection;
- Acid formation caused degradation of carbon fiber anode. The rate of acid formation depended on the current density. Lower current density produced less hydrogen and therefore led to less damage to the carbon fiber anode;
- Ions migration under the applied current changed the microstructure at the anode-paste interface, which was also influenced by the current density. Stronger current density may lead to faster migration or larger affected zone around the anode;

- Inhomogeneity of cementitious material could play a role in current distribution and damage pattern.

Chapter 8

Recommendations for future work

Based on the literature study and the outcomes of this work, the following future work can be recommended.

- Upper and lower limit of current density for CPre system

  As mentioned previously, the estimation was based on the hypothesis that 2.0 mA/m^2 of steel surface is sufficient to prevent steel reinforcement from corrosion initiation. Further study of chloride ingress profiles and chloride threshold concentration for initiation of corrosion under different current densities should be carried out in order to optimize the current density for safe prevention of reinforcement steel under the designed service life.

- Further experiments with increased number of specimens

  In order to remedy the randomness caused by inhomogeneity and improve the precision of the test results, further experiments with increased number of specimens are needed.

- Concrete behavior

  Due to the time limit, only paste and mortar material were investigated. In the future work concrete specimens should also be tested under the conditions of both accelerated high-current density and long-term low-current density.

- Field applications

  Field experiments or trails in a relatively large scale close to the real exposure are needed in the future in order to examine the practical applicability of this innovative prevention technique under the actually variable climate, such as wind, moisture changes, temperature changes and so on.

- Mathematical description and numerical modelling

  Besides lab and field experiments, numerical modelling is recommended as a complimentary design tool. Numerical modelling can provide more detailed

information about current distributions of the cathodic prevention system, taking into consideration of environmental factors, internal defects and other important factors.

- Improved approach of service life prediction

  Combining more accelerated test results, field data and numerical modelling, a better approach for prediction of service life of anode is expected. A more close-to-reality prediction would provide useful information for engineering design.

Bibliography

Ahmad, Zaki (2006). *Principles of corrosion engineering and corrosion control*. Burlington, Mass; Oxford, U.K: Butterworth-Heinemann (cit. on pp. 2, 4).

Bastidas, D. M., A. Cobo, E. Otero, and J. A. González (2008). "Electrochemical rehabilitation methods for reinforced concrete structures: advantages and pitfalls". In: *Corrosion Engineering, Science, and Technology* 43.3, pp. 248–255 (cit. on p. 2).

Bazzoni, A, Bruno Bazzoni, Luciano Lazzari, L Bertolini, and P Pedeferri (1996). *Field application of cathodic prevention on reinforced concrete structures*. Tech. rep. NACE International, Houston, TX (United States) (cit. on p. 4).

Bazzoni, Bruno, Atef Cheaitani, Philip Karajaili, Ray Dick, and Pietro Pedeferri (2006). "Performance of Cathodic Prevention System of Sydney Opera House Underbroadwalk After 10 Years of Operation". In: *CORROSION NACExpo 2006, 61st Annual Conference & Exposition* (cit. on p. 4).

Bertolini, L., F. Bolzoni, A. Cigada, T. Pastore, and P. Pedeferri (1993). "Cathodic protection of new and old reinforced concrete structures". In: *Corrosion Science* 35.5–8, pp. 1633–1639 (cit. on p. 4).

Bertolini, L, F Bolzoni, P Pedeferri, and T Pastore (1997). *Three year tests on cathodic prevention of reinforced concrete structures*. Tech. rep. NACE International, Houston, TX (United States) (cit. on p. 4).

Bertolini, L, F Bolzoni, P Pedeferri, L Lazzari, and T Pastore (1998). "Cathodic protection and cathodic preventionin concrete: principles and applications". In: *Journal of applied electrochemistry* 28.12, pp. 1321–1331 (cit. on pp. 2, 4).

Bertolini, L., F. Bolzoni, M. Gastaldi, T. Pastore, P. Pedeferri, and E. Redaelli (2009). "Effects of cathodic prevention on the chloride threshold for steel corrosion in concrete". In: *Electrochimica Acta* 54.5, pp. 1452–1463 (cit. on pp. 2, 3).

Bertolini, Luca, Fabio Bolzoni, Tommaso Pastore, and Pietro Pedeferri (2004). "Effectiveness of a conductive cementitious mortar anode for cathodic protection of steel in concrete". In: *Cement and Concrete Research* 34.4, pp. 681–694 (cit. on p. 4).

Chadwich, Z. Chaudhary; J. R. (1997). *Cathodic Protection of Buried Reinforced Concrete Structures*. Maney Publishing (cit. on p. 2).

Chang, JJ (2002). "A study of the bond degradation of rebar due to cathodic protection current". In: *Cement and concrete research* 32.4, pp. 657–663 (cit. on p. 7).

Chaudhary, Zia (2002). "Cathodic Prevention of New Seawater Concrete Structures in Petrochemical Plants". In: *CORROSION 2002* (cit. on p. 4).

Darowicki, K., J. Orlikowski, S. Cebulski, and S. Krakowiak (2003). "Conducting coatings as anodes in cathodic protection". In: *Progress in Organic Coatings* 46.3, pp. 191–196 (cit. on p. 4).

Dreyman, Edgar W (1972). "Precious metal anodes-state of art". In: *Materials Protection and Performance* 11.9, p. 17 (cit. on p. 4).

Eichler, T., B. Isecke, G. Wilsch, S. Goldschmidt, and M. Bruns (2010). "Investigations on the chloride migration in consequence of cathodic polarisation". In: *Materials and Corrosion* 61.6, pp. 512–517 (cit. on p. 3).

Enos, DG, AJ Williams Jr, and JR Scully (1997). "Long-term effects of cathodic protection on prestressed concrete structures: hydrogen embrittlement of prestressing steel". In: *Corrosion* 53.11, pp. 891–908 (cit. on p. 3).

Heidersbach, R.H., J. Brandt, D. Johnson, J.S. Smart III, and J.S. Smart (2006). "Marine Cathodic Protection, ASM Handbook". In: vol. 13C. ASM International. Chap. Corrosion: Environments and Industries, pp. 73–78 (cit. on p. 4).

ISO-12696 (2012). *Cathodic Protection of Steel in Concrete* (cit. on pp. 1, 2, 5).

Jing, Xu and Yao Wu (2011). "Electrochemical studies on the performance of conductive overlay material in cathodic protection of reinforced concrete". In: *Construction and Building Materials* 25.5, pp. 2655–2662 (cit. on p. 4).

Jochum, Klaus Peter, Ulrike Weis, Brigitte Stoll, Dmitry Kuzmin, Qichao Yang, Ingrid Raczek, Dorrit E Jacob, Andreas Stracke, Karin Birbaum, and Daniel A Frick (2011). "Determination of reference values for NIST SRM 610–617 glasses following ISO guidelines". In: *Geostandards and Geoanalytical Research* 35.4, pp. 397–429 (cit. on p. 19).

Kessler, Rechard J and Rodney G Powers (1989). "Conductive rubber as an impressed current anode: cathodic protection of steel-reinforced concrete". In: *Materials performance* 28.9, pp. 24–27 (cit. on p. 4).

Mahdi, Chini (2010). "Pan-based carbon fiber as anode material in cathodic protection systems for concrete structures". PhD thesis. Norwegian university of science and technology (cit. on p. 4).

Mayer, S. (2004). "Cathodic protection investigations into the effectiveness of a cathodic protection system for reinforced concrete specimens in order to optimize anode fields". PhD thesis. Munich university of applied science (cit. on p. 4).

Miranda, J. M., J. A. González, A. Cobo, and E. Otero (2006). "Several questions about electrochemical rehabilitation methods for reinforced concrete structures". In: *Corrosion Science* 48.8, pp. 2172–2188 (cit. on p. 2).

Miranda, J. M., A. Cobo, E. Otero, and J. A. González (2007). "Limitations and advantages of electrochemical chloride removal in corroded reinforced concrete structures". In: *Cement and Concrete Research* 37.4, pp. 596–603 (cit. on p. 2).

Mork, J.H., S. Mayer, and K. Rosenbom (2006). "Cathodic protection of concrete structures with a carbon fiber mesh anode". In: *EUROCORR2006*. Maastricht, the Netherlands (cit. on p. 4).

Mork, J.H., S. Mayer, and R. Asheim (2007). "Efficacite de la protection cathodique dans le port et sur la jetee de Honningsvag en Norvege". In: *ACTES DE LA 5E CONFERENCE INTERNATIONALE SUR LES STRUCTURES EN BETONS SOUS CONDITIONS*

EXTREMES D'ENVIRONNEMENT ET DE CHARGEMENT, CONSEC'07, TOURS, 4-6 JUIN 2007. Vol. 1 (cit. on p. 4).

NACE, Standard (1990). "RP0290-90 Standard Recommended Practice - Cathodic Protection of Reinforcing Steel in Atmospherically Exposed Concrete Structures". In: *Cathodic protection of reinforcing steel in atmospherically exposed structures* (cit. on p. 1).

Orellan, JC, G Escadeillas, and G Arliguie (2004). "Electrochemical chloride extraction: efficiency and side effects". In: *Cement and concrete research* 34.2, pp. 227–234 (cit. on p. 3).

Park, Ji Hoon and Jong Myung Park (2014). "Photo-generated cathodic protection performance of electrophoretically Co-deposited layers of TiO2 nanoparticles and graphene nanoplatelets on steel substrate". In: *Surface and Coatings Technology* 258, pp. 62–71 (cit. on p. 4).

Pedeferri, Pietro (1996). "Cathodic protection and cathodic prevention". In: *Construction and Building Materials* 10.5, pp. 391–402 (cit. on pp. 2, 3).

Peelen, WHA, RB Polder, E Redaelli, and L Bertolini (2008). "Qualitative model of concrete acidification due to cathodic protection". In: *Materials and corrosion* 59.2, pp. 81–89 (cit. on p. 3).

Polder, Rob B (1998). "Cathodic protection of reinforced concrete structures in The Netherlands-experience and developments". In: *BOOK-INSTITUTE OF MATERIALS* 710, pp. 172–183 (cit. on p. 2).

Polder, Rob B., Greet Leegwater, Daniël Worm, and Wim Courage (2014). "Service life and life cycle cost modelling of cathodic protection systems for concrete structures". In: *Cement and Concrete Composites* 47, pp. 69–74 (cit. on p. 3).

Rob, B. Polder and H. A. Peelen Willy (2011). "Service life aspects of cathodic protection of concrete structures". In: *Concrete Repair*. CRC Press, pp. 117–136 (cit. on p. 4).

Ryu, Jae-Suk, Nobuaki Otsuki, and Hiroshi Minagawa (2002). "Long-term forecast of Ca leaching from mortar and associated degeneration". In: *Cement and concrete research* 32.10, pp. 1539–1544 (cit. on p. 23).

Schreyer, Ch. Haldemann; A. (1997). "Ten Years of Cathodic Protection in Concrete in Switzerland". In: *Corrosion of Reinforcement in Concrete - Monitoring, Prevention and Rehabilitation: (EFC 25)*. Maney Publishing (cit. on p. 2).

Sergi, G, CL Page, and DM Thompson (1991). "Electrochemical induction of alkali-silica reaction in concrete". In: *Materials and Structures* 24.5, pp. 359–361 (cit. on p. 3).

Silva, Nelson, Luping Tang, and Sebastien Rauch (2013). "Application of LA-ICP-MS for meso-scale chloride profiling in concrete". In: *Materials and Structures* 46.8, pp. 1369–1381 (cit. on p. 20).

Tettamanti, M., A. Rossini, and Atef Cheaitani (1997). "CATHODIC PREVENTION AND CATHODIC PROTECTION OF NEW AND EXISTING CONCRETE ELEMENTS AT THE SYDNEY OPERA HOUSE". In: *CORROSION97* (cit. on p. 4).

Virmani, Yash Paul and Gerardo G Clemena (1998). *Corrosion Protection-Concrete Bridges*. Tech. rep. FHWA-RD-98-088, Final Report. Federal Highway Administration (cit. on p. 2).

Appendix

This appendix includes the results of LA-ICP-MS line scanning on control samples.

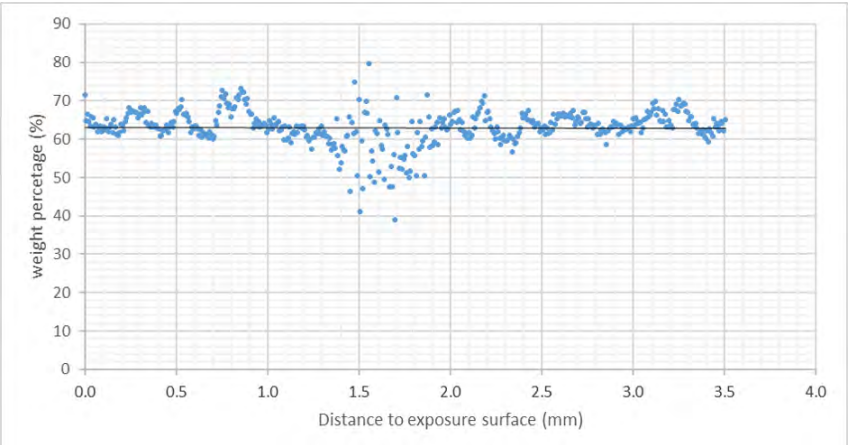

Figure 8.1: CaO baseline at approximately 64% of mass cement

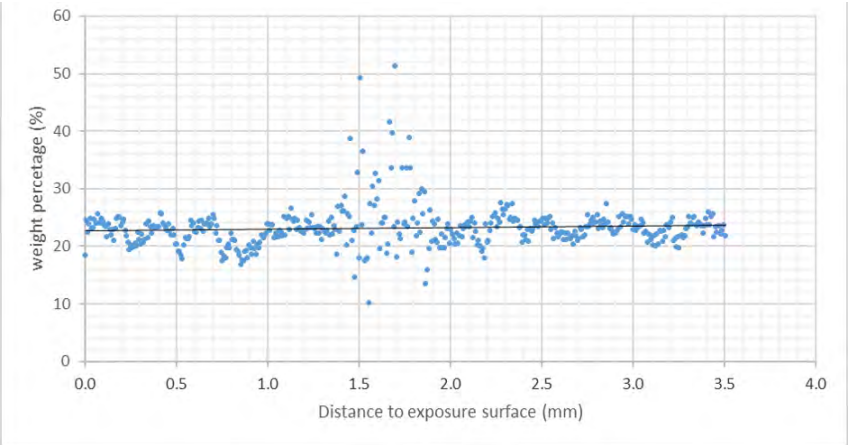

Figure 8.2: SiO_2 baseline at approximately 24% of mass cement

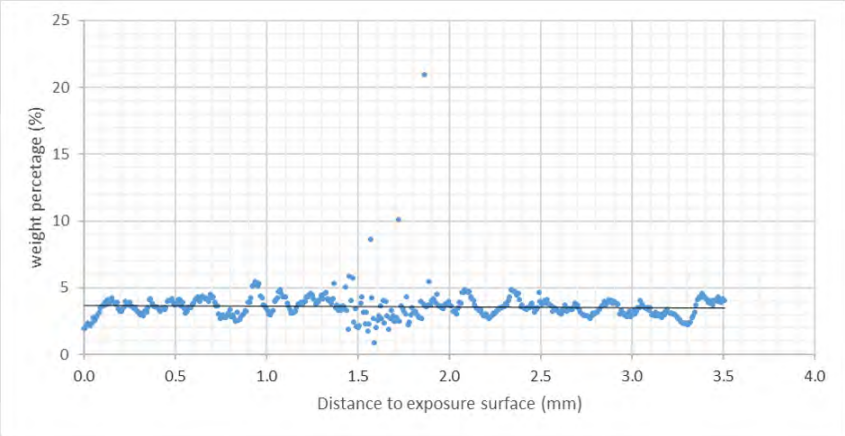

Figure 8.3: Al_2O_3 baseline at approximately 3.5% of mass cement

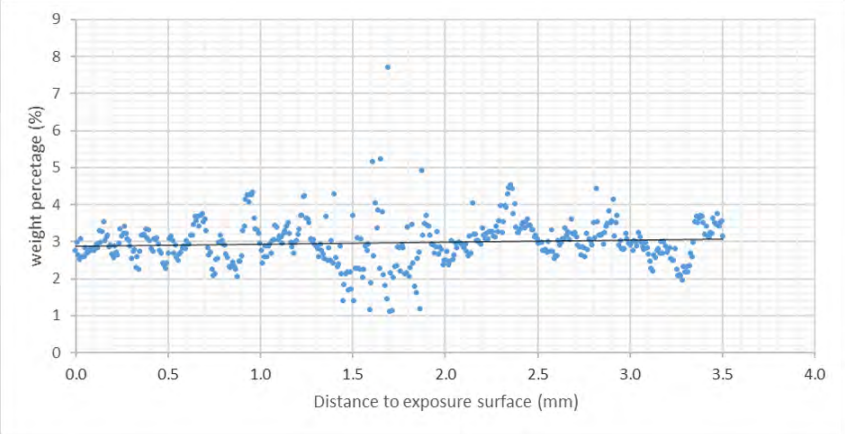

Figure 8.4: Fe_2O_3 baseline at approximately 3.0% of mass cement

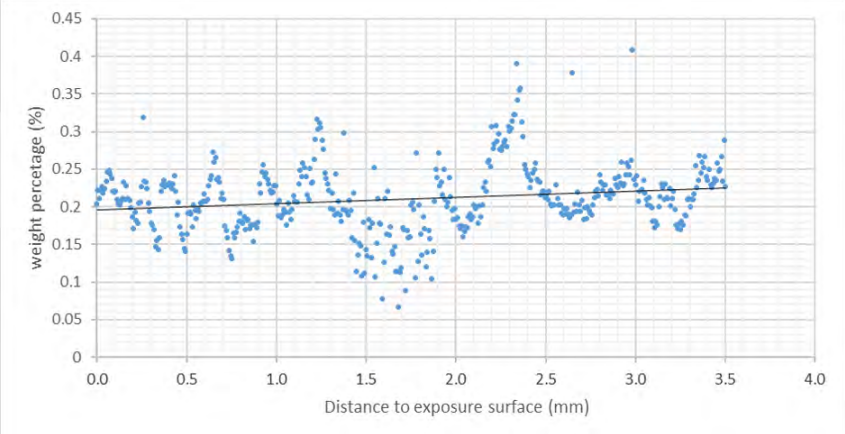

Figure 8.5: MgO baseline at approximately 0.23% of mass cement

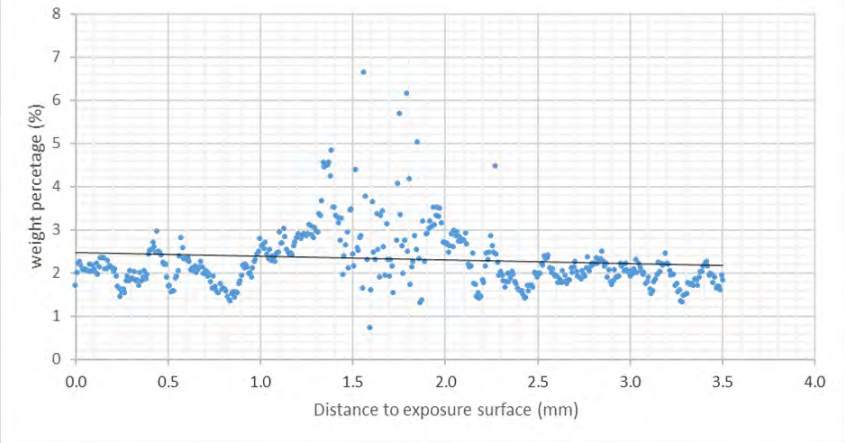

Figure 8.6: Na_2O baseline between 2.2-2.5% of mass cement

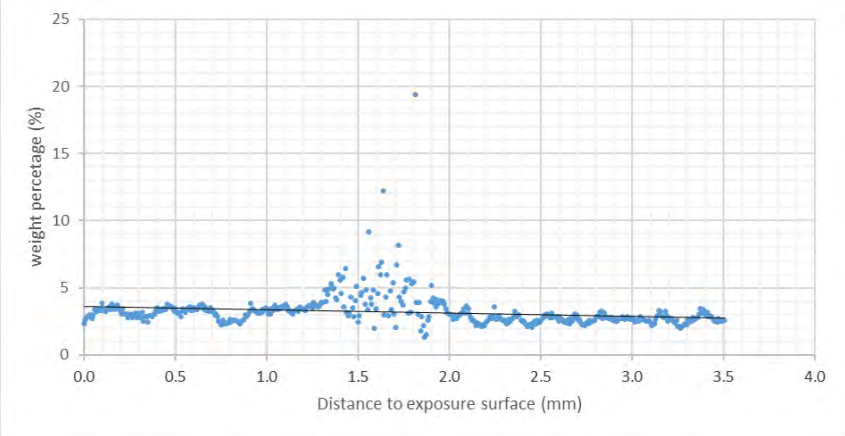

Figure 8.7: Cl baseline at approximately 3.4% of mass cement

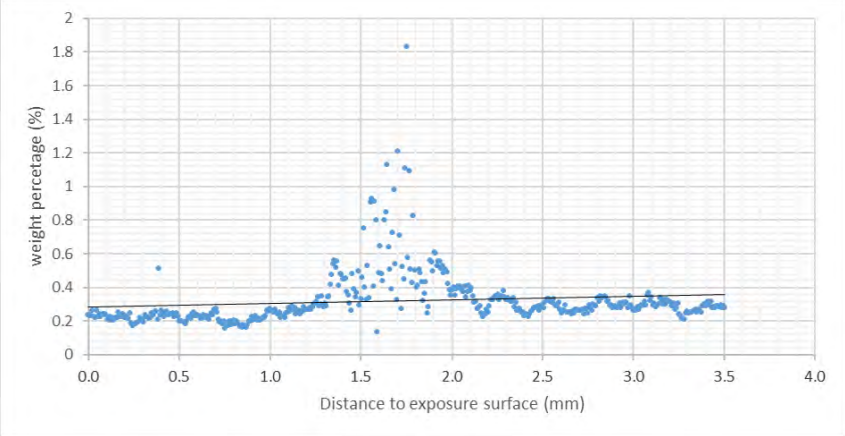

Figure 8.8: K_2O baseline at approximately 0.3% of mass cement